Desalination and Water Treatment
www.deswater.com

doi: 10.1080/19443994.2013.847805

53 (2015) 1417–1429
February

Taylor & Francis
Taylor & Francis Group

Cadmium removal by activated carbon, carbon nanotubes, carbon nanofibers, and carbon fly ash: a comparative study

Fahad Abdulaziz Al-Khaldi[a], Basel Abu-Sharkh[a], Abdalla Mahmoud Abulkibash[c], Muataz Ali Atieh[a,b,]*

[a]*Chemical Engineering Department, King Fahd University of Petroleum & Minerals, Dhahran 31261, Saudi Arabia*
Tel. +0096638607513; email: motazali@kfupm.edu.sa
[b]*Center of Research Excellence in Nanotechnology (CENT), King Fahd University of Petroleum & Minerals, Dhahran 31261, Saudi Arabia*
[c]*Chemistry Department, King Fahd University of Petroleum & Minerals, Dhahran 31261, Saudi Arabia*

Received 4 November 2012; Accepted 18 September 2013

ABSTRACT

Four types of carbonaceous adsorbent materials were applied for the removal of cadmium ions from water. These materials include fly ash (FA), activated carbon (AC), carbon nanofibers (CNFs), and carbon nanotubes (CNTs). The adsorption mechanisms and the kinetics of cadmium (II) removal from water were investigated. The effects of pH, the adsorbent dosage, the contact time, and the agitation speed on the removal process were studied and optimized. The four carbon adsorbents were characterized by field emission scanning electron microscopy and transmission electron microscopy. Adsorption isotherms were used to find the model of the adsorption behavior and to calculate the percentage removal. A 95% removal was obtained by using FA at pH 7, a dosage of 50 mg, a contact time of two hours, and an agitation speed of 150 rpm. In case of CNTs, CNFs, and AC, the percentage removals were found to be 27, 34, and 38%, respectively. The experimental data of the four-based carbon adsorbents were well fitted with Langmuir and Freundlich adsorption models.

Keywords: Activated carbon; Carbon nanotubes; Carbon nanofibers; Carbon fly ash; Cadmium removal

---

1. Introduction

Cadmium is a heavy metal that exists in natural deposits containing other elements. This element is highly toxic and considered as one of the major priority pollutants in drinking water. The World Health Organization (WHO) guidelines for Cd(II) content in water is 0.003 mg/L [1]. This stringent limit of cadmium in potable water is attributed to its severe toxicity, because it accumulates primarily in the kidneys. Moreover, its biological half-life of 10–35 years [1] in the human bodies is considered to be relatively long. As a drinking water pollutant, cadmium toxicity affects the kidneys. Cadmium metal is mainly used in steel and plastics industries. The industrial wastewater discharge of those activities is the main source of cadmium that reaches the environment. Other industrial sources of Cd(II) contamination include

---

*Corresponding author.

cooling tower blow down, electroplating, metal plating, coating operations, etc. Cadmium is also used in nickel–cadmium batteries, in Cd–Te thin film solar cells, and in pigments. Cadmium also exists as impurities in zinc that is used in the galvanized pipes and some metal fittings [2]. The common methods that are usually applied to control cadmium in the environment include: coagulation, ion-exchange, precipitation, softening, and membrane separation. Adoption of any of these technologies depends on the levels of the initial concentrations of cadmium as well as on the cost of each technology. Heavy metals are usually removed during the chemical and physical treatment processes of the raw water like seawater, brackish ground water, or surface water. However, in case, the limits set by WHO are exceeded, then the above-mentioned methods of water treatment could not be considered economically feasible. Such methods can be replaced by the adsorption method which is economically more feasible. Many adsorbents have been used to remove metal ions from wastewater including recycled alum sludge [3], peanut hulls [4], resins [5], kaolinite [6], manganese oxides [7], zeolite [8], and biomaterials [9,10]. However, the removal efficiencies of the metal ions using these adsorbents are low. Zhu et al. studied peanut hull as an adsorbent material for the removal of copper from waste stream. This study showed that these materials has a capacity of 21.25 mg/g to adsorb copper at a temperature of 30˚C, a pH of 5.5, and a contact time of two hours. According to this study, the adsorption isotherm model follows the Langmuir Isotherm [11]. However, the removal efficiencies of these adsorbents are considered to be low. Carbon nanotubes (CNTs) and carbon nanofibers (CNFs) have unique properties that make them potentially useful in various applications such as nanotechnology, electronics, optics, water treatment, and other fields of material sciences. Since their discovery in 1991 [12], CNTs and CNFs have attracted considerable research interests due to their exceptional mechanical and electrical properties. These nanomaterials have high chemical stability and large specific areas [13]. Multiwalled carbon nanotubes (MWCNT) have been used for the removal of metal ions, such as lead, copper, silver, and nickel [14]. Li et al. have reported that CNTs as an adsorbent for cadmium have shown lower adsorption efficiency compared to other metals such as lead and copper. The removal efficiency of the CNTs as metal ion adsorbents has been found to be significantly influenced by the pH of the medium [15]. The applications of CNFs, fly ash (FA), and activated carbon (AC) as adsorbents of the heavy metals from water have not been thoroughly investigated. Afsin-Elbistan FA and Seyitomer FA have been applied as adsorbents for Cd(II) at a pH of 7.0 and an agitation speed of 100 rpm [16]. The reported adsorption capacities of these two mentioned adsorbents for Cd(II) have been found to be 98.43 and 65.24%, respectively. Bayat have compared the adsorption effectiveness of these two types of FA with that of the AC (untreated powder, 0.150–0.038 mm) derived from charcoal. He has found that both types of FA are as effective as AC in the removal of Cd(II) [17]. Two different Brazilian FA were also evaluated as adsorbents for the removal of Cd(II) from an aqueous solution [18]. Both types of FA were found to have high adsorption capacity for Cd(II) when allowed to reach a required equilibrium time. The reported adsorption capacities were found to range from 50 to 100% based on the zeolite treatment and the initial concentration of cadmium ions in the original solution. Visa and Duta reported that the adsorption isotherms for Cd(II) by these two types of processed ashes follow the Langmuir model with adsorption capacity that ranges from 57 to 195 mg/g [19]. It has been found that by modifying the FA surface with methylene blue in alkaline solution, the efficiency of Cd(II) removal has increased. This study has confirmed the Langmuir Isotherm model for the cadmium adsorption mechanism [19]. Hydari et al. have studied the removal of cadmium ions using two type of commercial AC and have achieved 100% removal of cadmium at a pH of 6. According to this study, the adsorption isotherms for both the modified AC and the commercial AC follow Langmiura and Freundlich model, respectively [20].

The potentialities of four carbon-based adsorbents, namely: FA, AC, carbon nanofibres (CNFs), and CNTs in the removal of cadmium have been investigated. Different aqueous solutions having low initial contaminations of cadmium have been prepared and used in this study. The effects of the pH, the dosage of the adsorbent, the agitation speed, and the contact time on the removal efficiency of cadmium have been studied and optimized.

2. Materials and methods

2.1. Production of CNTs

The experimental setup used to synthesize the MWCNT is similar to that reported by Muataz et al. [21–27]. The floating catalyst chemical vapor deposition reactor was used to produce the CNTs. The production of CNTs in the present work has been conducted in a horizontal tubular reactor. The horizontal reactor is made of a quartz tube of an internal diameter of 50 mm and a length of 900 mm.

This reactor was heated by silicon carbide heating element. In this study, benzene (C_6H_6 99.5% purity) was used as a hydrocarbon source, ferrocene ($FeC_{10}H_{10}$ 98% purity) as a catalyst, hydrogen gas as a carrier, and argon was used to flush the air from the system. Several experiments were performed at reaction temperatures ranging from 500 to 1,200°C. Other conditions like the reaction time (45 min) and the hydrogen flow rate (300 mL/min) were fixed.

The produced CNTs were characterized using field emission scanning electron microscopy (FE-SEM) and transmission electron microscopy (TEM) and the purity was measured by thermogravimetric analysis.

2.2. Carbon nanofibers

CNFs, CNF > 95%, were purchased from Nanostructured & Amorphous Materials, Inc. USA. The length of these CNFs is in the range 10–40 μm, their outside diameters are in the range 200–500 nm, while the inside diameters are in the range 1–10 nm.

2.3. Activated carbon

The AC used in this study was a commercial carbon, CalgonFiltrasorb 400, and it was supplied in 10–30 mesh (1.00–0.60 mm) size. The granular AC was milled in a hammer cutter mill to form a powder of AC of a particle size $\leqslant$0.18 mm and it was used as an adsorbent for cadmium. The physical and chemical properties of the AC (Filtrasorb 400) are shown in Table 1.

The surface area of the AC was measured by nitrogen adsorption at 77 K using a Micromeritics Gemini 2,375 surface area analyzer (Micromeritics, Norcross, GA) and using a 15-point BET.

2.4. Fly ash

FA is one of the residues generated in the combustion process of coal and liquid fuels and represents the fine particles that rise with the flue gases. The FA used in this study was produced by burning heavy fuel oils in one of Saudi Aramco main power plants and the produced ash contains high percentage of unburned carbon and some other metals. Saudi Aramco produces hundreds of thousands of tons of FA per year. The FA was analyzed by the energy dispersive X-ray (EDX) to identify its elemental composition. The EDX analysis of the FA indicates that carbon represents a 67.56% of its weight beside many other different metals as is shown in the EDX spectrum (Table 2).

Table 1
The physical and chemical properties of the AC

Property	Value
Activated carbon	Filtrasorb 400
Surface area (M^2/g)	1,000
Bulk density	0.44 ± 0.003
Ash content (%)	8.3 ± 0.8
pH	7.9 ± 0.5
Attrition (%)	10.8 ± 3.2
Conductivity (μS)	4.7 ± 2.8

Recent concerns regarding environment awareness and the tighter regulations regarding the emission limits have forced people to utilize the FA produced. Most of the current research is trying to apply the FA as an additive to the Portland cement in order to increase the corrosion resistance of this cement. In this work, the FA, an adsorbent of low cost, was used in water treatment.

2.5. Stock solutions

The laboratory glass ware was rinsed with a solution of 2% nitric acid. This step is very important to remove all impurities from the glassware and to prevent further adsorption of cadmium (II) on the walls of the glassware. A cadmium stock solution of 1,000 mg/L was prepared. The stock solution was prepared by adding 2 mL of cadmium (II) standard solution which is of concentration 1,000 mg/L into the volumetric flask (2 L). Then, deionized water was added up to the mark and mixed thoroughly using a magnetic stirrer. The pH of the stock solution was adjusted by adding either a solution of 1.0 M nitric acid or a solution of 1.0 M NaOH. Finally, the buffer solutions were added to maintain constant pH during the experiment.

2.6. Batch mode adsorption experiment

Experiments of batch mode adsorption were conducted at room temperature to study the effect of the initial pH of the solution, the CNTs dosage, the contact time, and the agitation speed on the adsorption of Cd(II) ions. Each experiment was conducted in a volumetric flask and the initial and final concentrations of Cd(II) were analyzed using inductively coupled plasma-mass spectroscopy.

The percentage removed of Cd ions from the solution was calculated using the following relationship:

$$\%\ \text{Removal} = \frac{C_i - C_e}{C_i} \times 100 \tag{1}$$

The metal adsorption capacity (q_e) was calculated by the following equation:

Table 2
The EDX analysis of FA

Spectrum	C	O	Na	Mg	S	V	Fe	Ni	Cu	Zn	Total
% Components	67.562	3.73	0.12	2.04	4.98	0.76	0.12	0.25	0.25	0.19	100.0

$$\text{Adsorption capacity } (q_e) = \frac{C_i - C_e}{M_S} \times V(\text{mg/g}) \quad (2)$$

where C_i is the initial concentration of the metal ion in the solution (mg/L), C_e is the equilibrium concentration (mg/L), V is the total volume of solution (L), and M_s is the carbon dosage (g).

2.7. Adsorption isotherms model

Adsorption isotherms are mathematical models that describe the distribution of the adsorbate species between the liquid and the adsorbent. These models are established based on a set of assumptions that are mainly related to heterogeneity/homogeneity of adsorbents, type of coverage, and possibility of interaction between adsorbate species. The Langmuir model assumes that there is no interaction between the adsorbate molecules and the adsorption is localized in a monolayer. The Freundlich isotherm model is an empirical relationship describing the adsorption of solutes from a liquid to a solid surface and assumes that different sites with several adsorption energies are involved. In order to model the adsorption behavior and calculate the adsorption capacity of the adsorbents, the adsorption isotherms were studied. The Langmuir adsorption isotherm is perhaps the best known of all isotherms describing adsorption and is often expressed as:

$$Q_e = X_m K C_e/(1 + K C_e) \quad (3)$$

where Q_e: adsorption density at the equilibrium solute concentration C_e: (mg of adsorbate per g of adsorbent), C_e: equilibrium adsorbate concentration in solution (mg/L), X_m: the maximum adsorption capacity corresponding to complete monolayer coverage (mg of solute adsorbed per g of adsorbent), and K: the Langmuir constant related to the energy of adsorption. The above equation can be rearranged to the following linear form:

$$C_e/Q_e = 1/X_m K + C_e/X_m \quad (4)$$

The linear form can be used for linearization of experimental data by plotting C_e/Q_e vs. C_e. The Langmuir constants X_m and K can be evaluated from the slope and the intercept of the linear equation. In case of a good linearity fit, the adsorption can be described by the Langmuir isotherm. If the adsorption mechanism is not monolayer that can be described by Langmuir isotherm, then the Freundlich isotherm will be attempted:

$$Q_e = K_F C_e^{1/n} \quad (5)$$

where Q_e is the adsorption density (mg of adsorbate per g of adsorbent), C_e is the concentration of adsorbate in solution (mg/L), K_F and n are empirical constants which are dependent on several environmental factors and n are greater than one. This equation is conveniently used in the linear form by taking the logarithm of both sides as

$$\ln(Q_e) = \ln(K_F) + 1/n \ln(C_e) \quad (6)$$

A plot of $\ln(C_e)$ against $\ln(Q_e)$ yields a straight line which indicates that the adsorption is Freundlich isotherm. The constants can be determined from both the slope and the intercept.

2.8. Kinetic modeling

The study of sorption kinetics describes the adsorbate uptake rate and this rate evidently controls the residence time of adsorbate at the solid–liquid interface. In order to evaluate the mechanism of desorption of Cd(II) by each absorbent, the first-order equation, the pseudo-second-order rate equation, and the second-order rate equation are calculated by the following equations, respectively:

$$\text{Log}(q_e - q_t)/q_e = -K_L t/2.303 \quad (7)$$

$$t/q_t = 1/(2K_s q_e^2) + t/q_e \quad (8)$$

$$1/(q_e - q_t) = 1/q_e + kt \quad (9)$$

where q_e: sorption capacity at equilibrium, q_t: sorption capacity at time t (mg/g), K_L: the Lagergren rate constant of adsorption (1/min), k: rate constant of the pseudo-second-order sorption ($\text{g}\,\text{mg}^{-1}\,\text{min}^{-1}$), t: time (min). q_e, K_L, and k can be determined from the slopes and intercepts of the linear plots of log $(q_e - q_t)$ vs. t, t/q_t vs. t, and $1/(q_e - q_t)$ vs. t of the above equations.

3. Results and discussion

3.1. Characterization of the carbon-based adsorbents by SEM and TEM

The produced CNTs, CNFs, AC, and FA were characterized by SEM and TEM. Fig. 1 shows the SEM images of CNTs, CNFs, AC, and FA, respectively. The diameters of the produced CNTs vary from 20 to 40 nm with an average diameter of 24 nm while the average diameter of CNFs varies from 100 to 250 nm. The size of AC varies in the range 600–1,000 micron, while in case of FA its size varies in the range 500–1,500 micron. The SEM image of FA compared to the AC demonstrates the high surface area of the FA and its potentiality as an adsorbent. One important feature of FA over other carbon-based adsorbents is the high

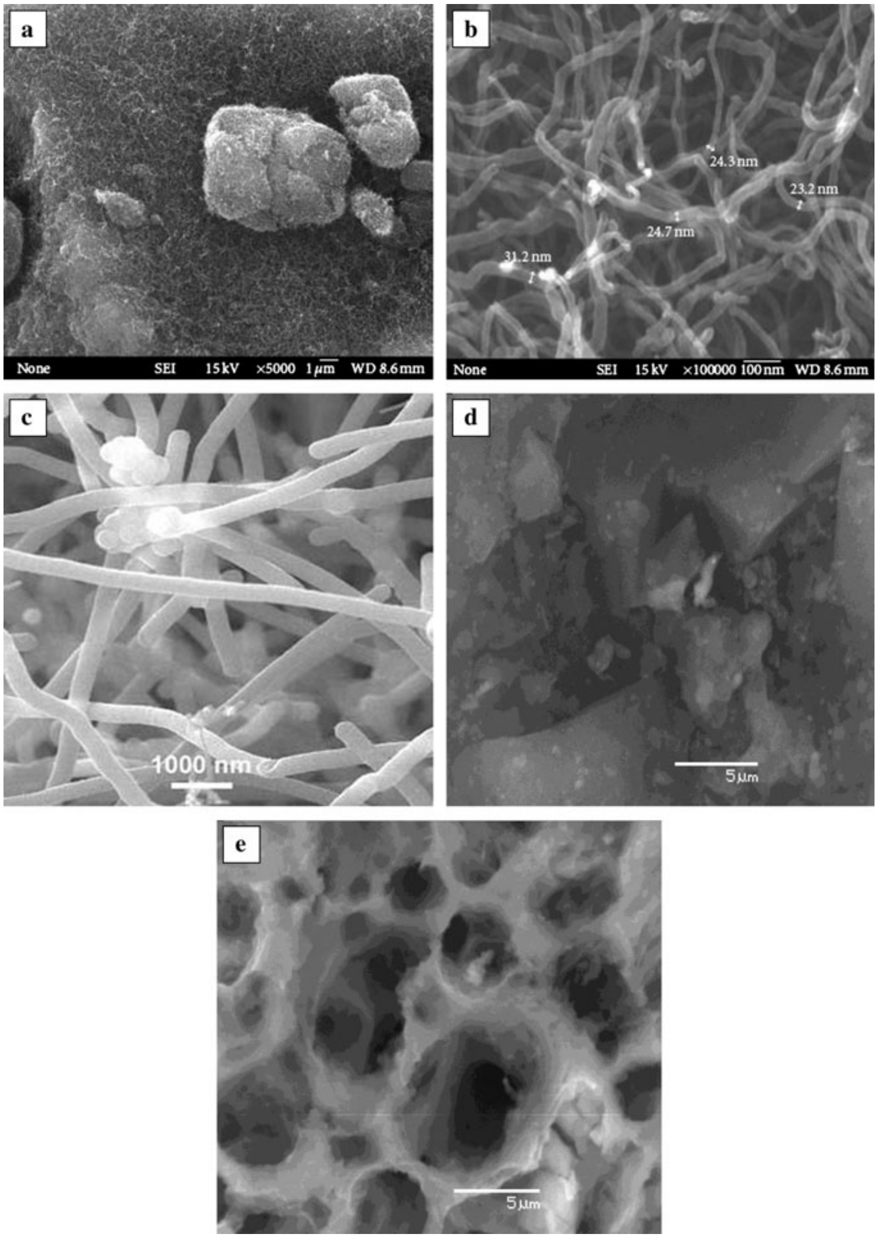

Fig. 1. SEM images: (a) and (b) CNTs, (c) CNFs, (d) AC, and (e) FA.

contents of metals which help in enhancing the adsorption process.

TEM which is usually used to characterize the structure of the nanomaterials was applied to characterize the structure of the CNTs and the CNFs (Fig. 2). The size of each of the particles of AC and FA is of few hundred microns and cannot be characterized by TEM. To prepare the samples for TEM study, some drops of alcohol were put on films of nanotubes and then these films were transferred with a pair of tweezers to a carbon-coated copper grid. It is obvious from the images that all the nanotubes are hollow and tubular in shape. In some of the images, catalyst particles can be seen inside the nanotubes as well as in the nanofibers. Fig. 2(a) and (b) shows the TEM images of the CNTs. The TEM images indicate that the nanotubes are of high purity, with uniform diameter distribution and contain no deformity in the structure. Fig. 2(b) shows the images of the CNTs obtained by the high-resolution transmission electron microscope (HRTEM). A highly ordered crystalline structure of CNTs is observed. The clear fringes of graphitic sheets are well separated by 0.34 nm and aligned with a tilted angle of about 2° toward the tube axis. The HRTEM shows that the CNTs are of about 19 graphitic walls.

Fig. 2(c) and (d) shows the TEM image of CNFs. These figures show that the graphitic platelets are precipitated parallel to the surface of the faceted catalyst particle and hence the angle between the plane and the fiber axis is determined by the shape of the catalyst as shown in Fig. 2(c). It is clearly shown in Fig. 2(c) that the catalyst has two faces capable of dissociative chemisorbing of hydrocarbon molecules and four faces that simultaneously precipitate dissolved carbon as graphite platelets. It shows that the formation of the nanofiber is of bidirectional growth where the catalyst particles were embedded within the nanofiber structure. Fig. 2(d) shows the high magnification of TEM image of this nanofiber, the graphite platelets are oriented parallel to the surface of the catalyst. The nanofiber has herringbone structure.

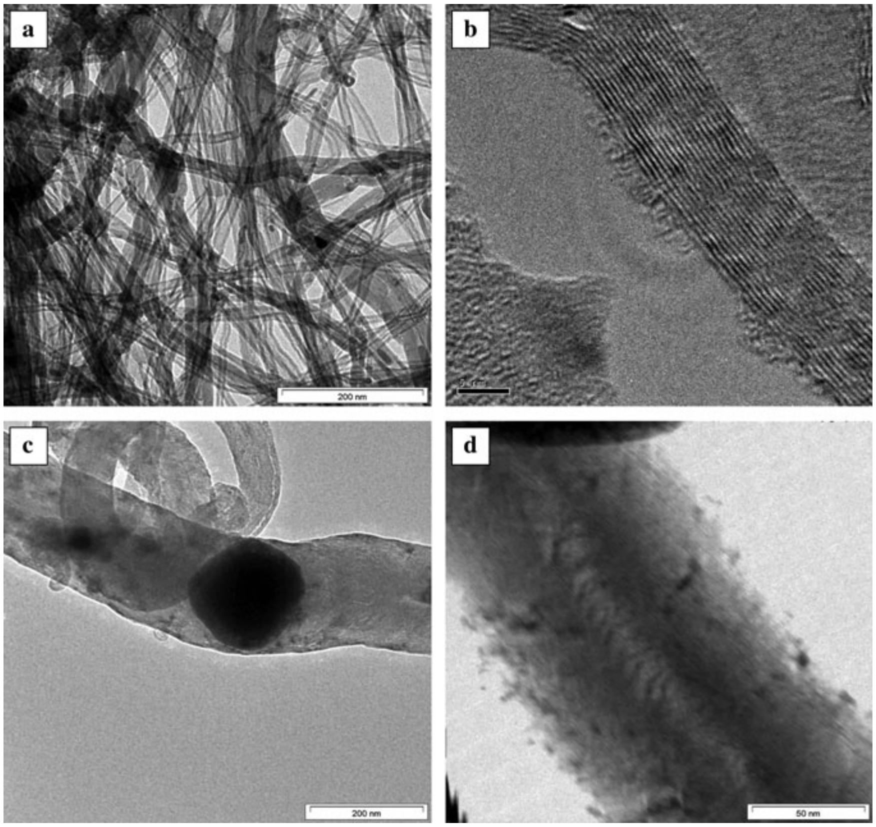

Fig. 2. TEM Images of CNTs: (a) at low resolution, (b) at high resolution and CNFs, (c) at low resolution, and (d) at high resolution.

3.2. Thermal analysis of carbonaceous adsorbents

The thermogravimetric (TG) and derivative thermogravimetric (DTG) curves obtained for the four adsorbents at heating rates of 10˚C/min are shown in Fig. 3(a)–(d). The TG thermgrams were carried out in air and it was noted that there was some residual remains of the samples, when it was heated to about 900˚C. For CNTs (Fig. 3(a)), the residue appears reddish which shows that all of the CNTs were oxidized leaving only the catalyst. It can be seen that this decomposition process is a single-stage decomposition reaction where the procedural decomposition temperatures are well defined. The initial degradation temperature (T_i) for the CNT occurs at 520˚C while the maximum weight loss was found to be at (T_m) 650˚C and the final degradation temperature was (T_f) 740˚C. For CNFs (Fig. 3(b)), two peaks have been observed; this is due to the wide difference in the sizes of CNFs. The CNFs with small diameters decompose first at 500˚C while that of the large diameters takes longer time to decompose at 720˚C and shows a second peak in the thermogram. AC (Fig. 3(c)) apparently contains volatile materials that burn off during the initial heating process while the metal impurities remain after the completion of the heating process. FA, in contrast, shows a mixture of different forms of carbon-based materials (Fig. 3(d)). The obtained TG thermgrams for the FA indicate that the used FA has three major components: volatile material (25% wt.), carbon-based material (35% wt.) and other material of high temperature resistance that include both the metals and other impurities.

3.3. Cadmium adsorption by the four different carbonaceous materials

3.3.1. Effect of pH

The pH was found to be a predominant factor affecting the removal of cadmium ions under the conditions studied. Cadmium species can be present in deionized water in the forms of Cd^{2+}, $Cd(OH)^+$, and $Cd(OH)2_{(s)}$ [28]. At low pH, the dominant cadmium species is Cd^{2+} which exists in the form of a complex $[Cd(H_2O)_6]^{2+}$ [28]. The removal of cadmium by the four adsorbents at various pH values has been studied and the results are shown in Fig. 4.

The variations of pH used in the experiments are within the range 2–8. The same phenomenon of the effect of pH was observed for the other adsorbents CNTs, CNFs, and AC. The removal of Cd(II) by CNTs, CNFs, and AC was found to increase by increasing the pH of the cadmium solutions from pH 4 to 7. There

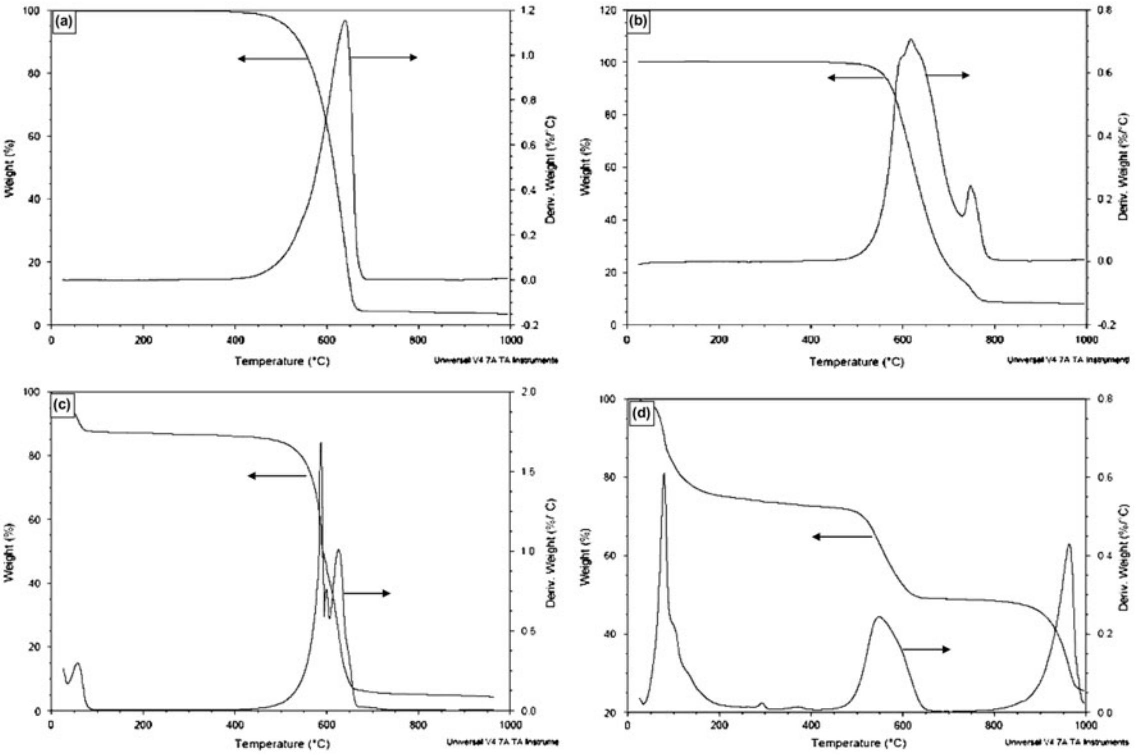

Fig. 3. TG curve (wt.%) and DTG curve (Derivative wt.%/˚C) for: (a) pure CNTs, (b) CNFs, (c) AC, and (d) FA.

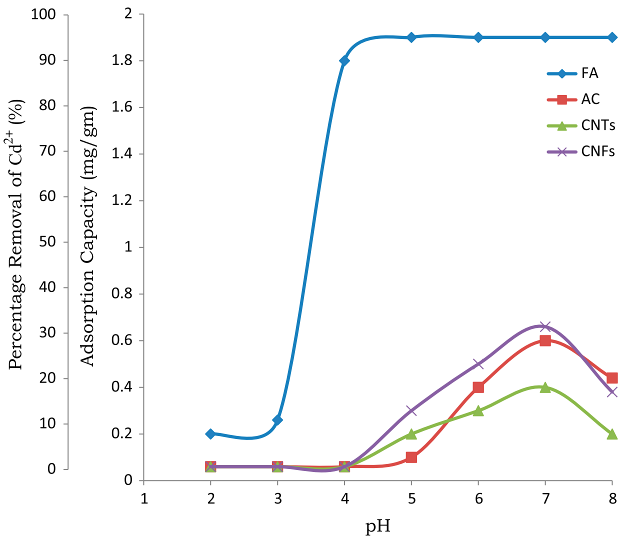

Fig. 4. The effect of pH on the percentage removal and adsorption capacity of cadmium.

was no removal of cadmium (Cd^{2+}) by these three adsorbents with each of the solutions' pH lower than 4. This is due to the strong competition between H^+ and Cd^{2+} ions on the adsorption sites [29]. However, the number of H^+ ions decreases on increasing the pH from 5.5 to 7.60 and this will in turn increase the adsorption of Cd^{2+}. In slightly alkaline solutions, the predominant ion will be the HCO_3^- ion [30]. At pH 7, the maximum percentage removal of cadmium, by CNTs, CNFs, and AC, was found to be 27, 34, and 38%, respectively. However, FA shows superior adsorption of Cd^{2+} ions from solutions of a pH range 4–7. The reported percentage removal of FA, as shown in Fig. 4, is 95% that is higher than adsorption capacities of the other three carbon-based adsorbents. At $pH > 6.0$, Cd^{2+} exists as Cd $(OH)_2$ while at $pH < 6.0$, this ion will be available as $Cd(OH)^+$ [31]. An increase in the metal adsorption from solutions of a pH greater than 6.0 is attributed to withholding of Cd $(OH)_2$ into the micropores of carbon particles. The superior cadmium removal by FA is attributed to the presence of many metals (Mg, V, Fe, Zn, Ni, and Cu) on the surfaces of Saudi Aramco FA. The presence of such metals will enhance the development of charges on the surface of the FA. Accordingly, electrostatic attractions will develop between the Cd(II) ions in the solutions and the surface of the FA [31].

3.3.2. Effect of agitation speed

The conditions that have resulted in the high adsorption capacity of Cd(II) at pH 7 were applied to study the effect of the agitation speed on the adsorption capacity of cadmium by the four adsorbents. It was observed that the adsorption capacity of Cd(II) increases when the speed of agitation was increased from 50 to 150 rpm in case of the four adsorbents as shown in Fig. 5. However, on increasing the agitation speed above 150 rpm, the adsorption capacity of the AC was only found to increase [31–33] while those of CNTs, CNFs, and FA have started to decline. An increase in the amount of dosage will furnish more exchangeable sites for ions. Thus, the adsorption capacity increases with adsorbent dosage up to the value of 50 mg. However, the increase of the dosage above this value has resulted in a steady state of the adsorption capacity. This indicates that the removal of Cd^{2+} is an equilibrium reaction. Agitation facilitates proper contact between the metal ions in solution and the adsorbents binding sites and thereby promotes effective transfer of cadmium ions to the carbon active sites and improves the diffusion of cadmium ions towards the surface of the adsorbents. The increased adsorption of Cd(II) by AC in case of agitation speeds above 150 rpm indicates the presence of small diameter sites in the AC that can become effective only at high flow speeds. According to Nomanhay and Palamisamy, the increase in agitation rate improves the diffusion of metal ions towards the adsorbent's surface [34].

3.3.3. Effect of contact time

The adsorption behavior of cadmium by these four adsorbents as a function of contact time was studied by varying the contact time from a period of 10 min to 24 h using a Cd^{2+} concentration of 1 mg/L, a dose of an adsorbent of 50 mg/L, and an optimum pH of 7. The agitation speed was fixed at 150 rpm thoroughout

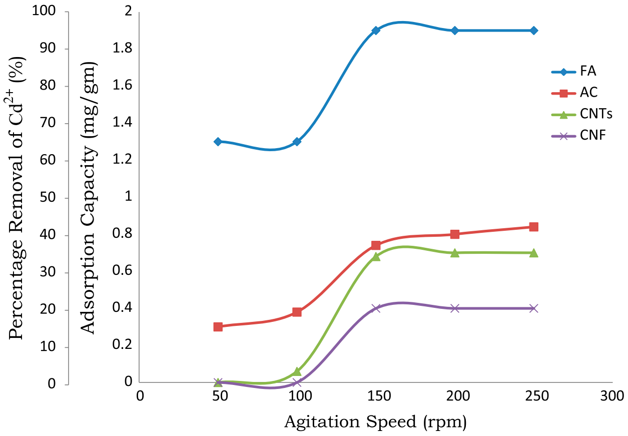

Fig. 5. The effect of agitation speed on the percentage removal of cadmium at pH 7.

the experiments. For each of the adsorbents, the adsorption rate reaches to equilibrium after two hours. For CNTs, CNFs, AC, and FA, the percentage removal of Cd^{2+} is 27, 34, 38, and 95%, respectively. In case of FA, the reaction is much faster because the adsorption sites are well exposed compared to other adsorbents, which show much lower capacity for adsorption. No further increase in the removal efficiency was observed with time for the adsorbents after a contact time of two hours except in case of AC. It is clear that the removal has increased even after a time of 24 h confirming the observation of the effect of agitation speed that indicates the presence of adsorption sites that are not readily accessible and require high agitation speed and long diffusion time to be accessed. According to Bhattacharyya and Gupta [35], the initial high rate of metal uptake may be attributed to the existence of the bare surface. The number of the available adsorption sites decreases as the number of Cd^{2+} ions adsorbed increases. The enhanced adsorption of metal with increase in agitation time may also be due to the decrease in boundary layer resistance in the kinetics energy of the hydrate layer (Fig. 6).

3.3.4. Effect of adsorbents dosage

The amount of adsorbents in water is considered as one of the major factors which affect the adsorption capacity. The batch adsorption experiments were carried out by using various amounts of FA, AC, CNFs, and CNTs from 25 to 250 mg while the pH, agitation speed, and contact time were fixed at 7, 150 rpm, and 120 min, respectively. The results shown in Fig. 7 indicate that the adsorption capacity increases with an increase of the adsorbent dosage up to 50 mg and then it becomes almost steady for the rest of the dosage range. For the range below 50 mg, the increase in percentage removal with the increase of the dosage is expected because the higher the dose of adsorbents in the solution, the greater the availability of exchangeable sites for ions. However, after certain dosage value, which is 50 mg in this study, the dosage amount was found to have no effect on the percentage removal. This would indicate that the Cd^{2+} removal is an equilibrium reaction and is not limited by the number of adsorption sites of the adsorbent up to the concentrations studied. It has been reported that the fraction of the cations adsorbed onto the oxide surfaces has increased from 0 to 1 over a narrow pH range of one pH unit and the pH edge shifts from left to right showing an increase of the adsorbate/adsorbent ratio [36].

3.4. Freundlich and Langmuir isotherms adsorption model

The *Freundlich and Langmuir isotherms* adsorption model are the most common model used to quantify the amount of adsorbate adsorbed on an adsorbent as a function of the partial pressure or the concentration at a given temperature. It considers adsorption of an ideal gas onto an idealized surface. Freundlich and Langmuir isotherms relate coverage or adsorption of molecules on a solid surface to gas pressure or concentration of a medium above the solid surface at a fixed temperature.

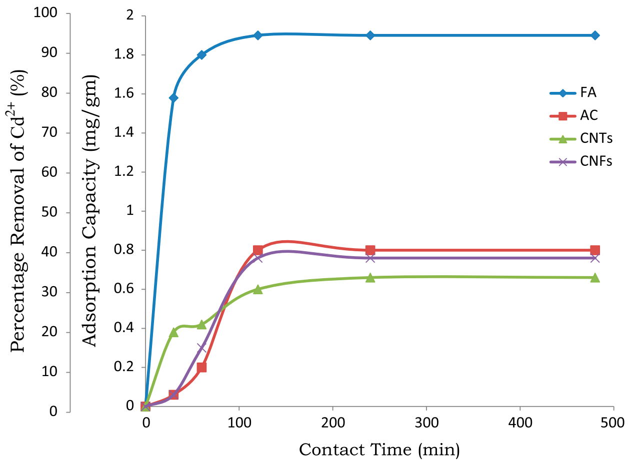

Fig. 6. The effect of contact time on the percentage removal of cadmium at 150 rpm at pH 7.

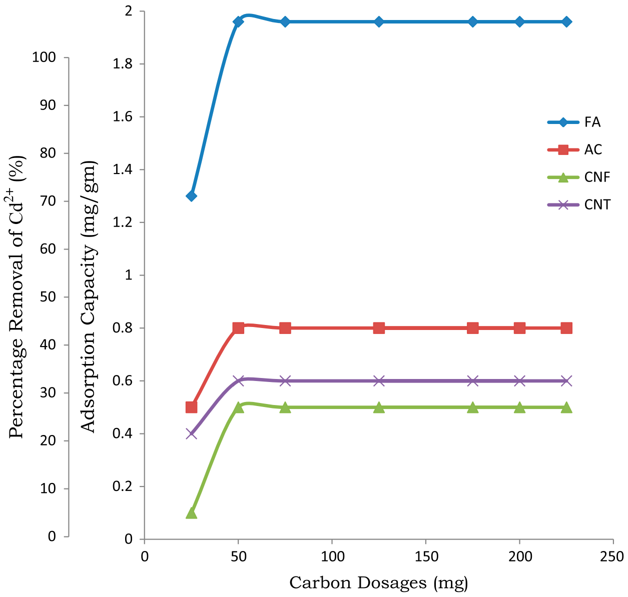

Fig. 7. The effect of adsorbents dosages on the percentage removal of cadmium at pH 7.

3.5. Langmuir and Freundlich adsorption isotherm models for cadmium

The equilibrium adsorption is important in the design of adsorption systems. Equilibrium studies in adsorption indicate the maximum capacity of the adsorbent during the treatment process. Taking into account that the percentage removal is the highest at pH 7, thus, the condition was used to further optimize the adsorption process parameters. The equilibrium curve was modeled in Fig. 8.

The Langmuir and Freundlich equations were used to describe the data derived from the adsorption of Cd(II) by the different adsorbents over the entire parameters range studied. Based on Fig. 9, the adsorption capacities (q_e) and adsorption intensities were determined from the slope and the intercept of each absorbent graph, respectively.

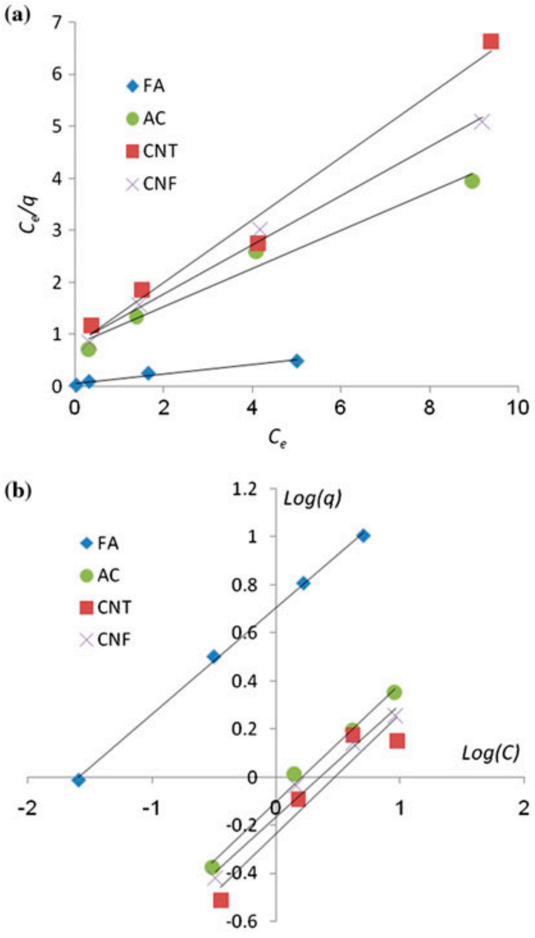

Fig. 8. Adsorption isotherm models for cadmium removal at pH 7: (a) Langmuir and (b) Freundlich.

On comparing Langmuir isotherms with that of Freundlich isotherms, Freundlich Isotherm shows better fitting model with higher correlation coefficients for the AC and FA; whereas the data for both nanocarbon types (CNTs and CNFs) are better represented by Langmuir Isotherm. However, the Freundlich isotherm applications for CNTs and CNFs are still within the acceptable range (above 90%); therefore, the applicability of monolayer coverage of Cd(II) ions on the surface of the four adsorbents is a valid assumption. This is due to the fact that all of the four adsorbents have great surface areas for metal adsorption. The above analysis also indicates that Cd (II) ions strongly adsorbed to the surfaces of these adsorbents suggesting that these forms of carbon-based adsorbents have great potential to be good adsorbents and can be applied for the removal of Cd (II) ions in water treatment.

From Table 3, it can be seen that FA has a greater adsorption capacity when compared to the other three adsorbents. Each gram of FA can uptake three to four times the absorbent capacity of other three adsorbents. This high adsorption capacity could be related to the high surface area but could be also explained by the metal content of the FA as suggested by Li et al. [15].

3.6. Modeling of kinetics adsorption

Modeling of kinetic data is fundamental for the industrial application of adsorption since it gives essential information required for a comparison

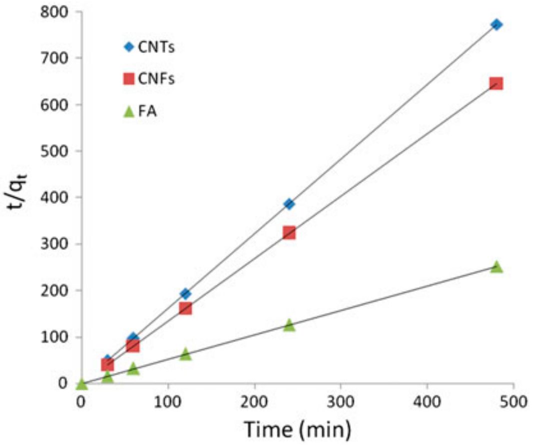

Fig. 9. Pseudo-second-order kinetics of Cd adsorption by CNTs, CNFs, and FA.

Table 3
Parameters of Langmuir and Freundlich adsorption isotherm models for cadmium removal

	Langmuir			Freundlich		
	q_m	K_L	R^2	n	K_F	R^2
CNT	1.661	0.761	0.979	2.008	0.791	0.912
CNF	2.123	0.555	0.993	2.141	0.851	0.982
AC	2.725	0.456	0.976	2.033	0.906	0.991
FA	11.23	1.435	0.968	2.247	2.028	0.998

among different adsorbing materials under different operational conditions. This type of comparison is important for designing and optimizing the operational conditions to be applied in the process of pollutant removal from wastewater systems [16].

The kinetics was investigated by using the information obtained from the effect of dosage (dry weight basis) at 25°C at several different time intervals up to 480 min. Table 4 shows the correlation coefficients for each model used to describe each of the four adsorbents. From Table 4, the first-order kinetic equation can be used to describe Cd^{2+} adsorption by AC; however, the pseudo-first-order kinetic equation was not applicable for CNTs, CNFs, and FA because R^2 for these adsorbents is small compared to R^2 of pseudo-second-order equation. Therefore, the pseudo-second-order equation was used in this study in order to investigate the mechanism of adsorption of Cd(II) by the three adsorbents and the potential rate controlling steps, such as mass transport and chemical reactions. The pseudo-second-order kinetic equation is:

$$dq_t/dt = k_2(q_e - q_t)^2 \tag{10}$$

where q_e and q_t are the sorption capacity (mg/g) at equilibrium and at time (t), respectively, and k_2 is the rate constant of the pseudo-second-order sorption (g mg^{-1} min^{-1}). For the boundary conditions $t = 0$ to $t = t$, $q_t = 0$ and $q_t = q_t$, the integrated form of (10) becomes:

Table 4
Correlation coefficients for kinetic models of cadmium adsorption by CNTs, CNFs, AC, and FA

Adsorbent (50 mg)	First-order	Pseudo-second order	Second-order
CNTs	0.974	0.999	0.809
CNFs	0.937	0.976	0.826
AC	0.956	0.725	0.913
FA	0.904	0.999	0.971

Table 5
Kinetic parameters for pseudo-second-order model of cadmium adsorptions by CNTs, CNFs, and FA

Adsorbent (50 mg)	q_e (mg/g)	K_2 (g mg^{-1} h^{-1})	R^2
CNT	0.657	0.028	0.999
CNF	0.840	0.010	0.976
FA	1.838	1.156	0.999

$$1/(q_e - q_t) = 1/q_e + k_2 t \tag{11}$$

This has a linear form:

$$1/q_t = 1/k_2 q_e^2 + t/q_e \tag{12}$$

The integrated form of the equation is

$$t/q_t = 1/h + (1/q_e)/t \tag{13}$$

where h (g mg^{-1} min^{-1}) can be regarded as the initial sorption rate $q_t/t \rightarrow 0$, hence $h = k_2 q_e{}^2$. If the pseudo-second-order kinetics is applicable to the experimental data, the plot of t/q_e vs. time of (13) gives a linear relationship from which q_e, k, and h can be determined from the slope and the intercept of the plot, respectively.

3.7. Kinetics adsorption model of cadmium (II)

Parameters of the kinetics adsorption model for cadmium (II) at pH 7 are shown in Table 5 for CNTs, CNFs, and FA. Plotting t/q_t vs. time (Fig. 9) yields very good straight lines. From the second-order rate constant, shown in Fig. 9 and Table 5, it can be concluded that the time to achieve equilibrium concentration of Cd(II) using FA is less than that required for both CNTs and CNFs. For the AC, it is best represented by the first-order equation with a correlation coefficient $R^2 = 0.956$.

The equilibrium adsorption capacity, q_e *is* obtained from the graph and Table 5 also implies that FA has much higher adsorption capacity ($q_e = 1.838$ mg/g), compared to the other adsorbents. AC still shows approximately equal adsorption capacity ($q_e = 0.8$ mg/g) when compared to nanocarbons.

4. Conclusion

Four types of carbonaceous adsorbent materials were found to be efficient for the removal of Cd(II) from aqueous solutions. Characterization of the Cd(II) uptake showed that cadmium ions binding is dependent on the initial pH, agitation speed, amount of dosage, contact time morphology of the surface, and metal content of the surface of adsorbents. Percentage uptake of Cd(II) increased with the pH from a value of 2–7. The optimum pH was found to be 7 that resulted in percentage removal of 30–40% removal of Cd(II) ions using regular CNTs, CNFs, and AC, respectively. However, the FA gives percentage removal of 95%. The percentage uptake increased slightly with an increase in agitation speed from 50 to 150 rpm, for which 150 rpm gave slightly higher removal for cadmium. While the percentage removal of Cd(II) was observed to increase with an increase in the adsorbent dosages, it was found that beyond 50 mg the dosage amount has no effect on the percentage removal of Cd ions under the conditions specified in this study.

Highest removal of cadmium ions was archived using FA as an adsorbent. The high removal of Cd(II) by FA is due to the strong tendency towards chemical bonding between the Cd(II) ions and the metals contained in the FA. One concern about FA is the fact that FA composition changes according to its source, therefore, the results of this study cannot be expected to all types of FA. FA was found to be a good candidate as Cd(II) adsorbent. FA is a waste material that could be used as a good adsorbent for water treatment. This should help in both improving the waste management and establishing a new low-cost water treatment material.

Acknowledgment

The author(s) would like to acknowledge the support provided by King Abdulaziz City for Science and Technology (KACST) through Science & Technology Unit at King Fahd University of Petroleum & Minerals (KFUPM) for funding this work through project No: 13-ADV161-04 as part of the National Science, Technology and Innovation Plan.

References

[1] World Health Organization Guidelines (2006). http://www.who.int/water_sanitation_health/dwq/gdwq3rev/en/

[2] Y. Li, S. Wang, Z. Luan, J. Ding, C. Xu, S. Wu, A desorption of cadmium (II) from aqueous solution by surface oxidized carbon nanotubes, Carbon 41 (2003) 1057–1062.

[3] W. Chu, Lead metal removal by recycled alum sludge, Water Res. 33(13) (1999) 3019–3025.

[4] P. Brown, I. Jefcoat, D. Parrish, S. Gill, E. Graham, Evaluation of the adsorptive capacity of peanut hull pellets for heavy metals in solution, Adv. Environ. Res. 4(1) (2000) 19–29.

[5] C. Diniz, F. Doyle, V. Ciminelli, Effect of pH on the adsorption of selected heavy metal ions from concentrated chloride solutions by the chelating resin Dowex M-4195, Sep. Sci. Technol. 37(14) (2002) 3169–3185.

[6] M. Arias, M. Barral, J.C. Mejuto, Enhancement of copper and cadmium adsorption on kaolin by the presence of humic acids, Chemosphere 48(10) (2002) 1081–1088.

[7] R. Sublet, M. Simonnot, A. Boireau, M. Sardin, Selection of an adsorbent for lead removal from drinking water by a point-of-use treatment device, Water Res. 37(20) (2003) 4904–4912.

[8] B. Biskup, B. Subotic, Removal of heavy metal ions from solutions using zeolites. III. Influence of sodium ion concentration in the liquid phase on the kinetics of exchange processes between cadmium ions from solution and sodium ions from zeolite A, Sep. Sci. Technol. 39(4) (2004) 925–940.

[9] Q. Li, S. Wu, G. Liu, X. Liao, X. Deng, D. Sun, Y. Hu, Y. Huang, Simultaneous biosorption of cadmium (II) and lead (II) ions by pretreated biomass of *Phanerochaete chrysosporium*, Sep. Purif. Technol. 34(1–3) (2004) 135–142.

[10] F. Ekmekyapar, A. Aslan, Y.K. Bayhan, A. Cakici, Biosorption of copper(II) by nonliving lichen biomass of Cladoniarangiformishoffm, J. Hazard. Mater. 137(1) (2006) 293–298.

[11] C. Zhu, L. Wang, W. Chen, Removal of Cu (II) from aqueous solution by agricultural by-product: Peanut hull, J. Hazard. Mater. 168(2–3) (2009) 739–746.

[12] S. Iijima, Helical microtubules of graphitic carbon, Nature 354 (6348) (1991) 56–58.

[13] S. Haddon, Carbon nanotubes, Acc. Chem. Res. 35(12) (2002) 977–1113.

[14] A. El-Sheikh, Effect of oxidation of activated carbon on its enrichment efficiency of metal ions: comparison with oxidized and non-oxidized multi-walled carbon nanotubes, Talanta 75(1) (2008) 127–134.

[15] Y. Li, J. Ding, Z. Luan, Z. Di, Y. Zhu, C. Xu, D. Wu, B. Wei, Competitive adsorption of Pb^{2+}, Cu^{2+} and Cd^{2+} ions from aqueous solutions by multiwalled carbon nanotubes, Carbon 41(14) (2003) 2787–2792.

[16] B. Nowak, P. Aschenbrenner, F. Winter, Heavy metal removal from sewage sludge ash and municipal solid waste fly ash – A comparison, Fuel Process. Technol. 105(1) (2013) 195–201.

[17] B. Bayat, Comparative study of adsorption properties of Turkish fly ashes: The case of chromium (VI) and cadmium (II, J. Hazard. Mater. B 95 (2002) 275–290.

[18] J. Izidoro, A. Fungaro, E. Abbott, S. Wang, Synthesis of zeolites X and A from fly ashes for cadmium and zinc removal from aqueous solutions in single and binary ion systems, Fuel 103 (2013) 827–834.

[19] M. Visa, A. Duta, Cadmium and copper removal from aqueous solution by adsorption onto treated fly ash collected from Cet-Brasov, Bull. Transilvania Univ. Brasov 50(1) (2008) 293–305.

[20] S. Hydari, H. Sharififard, M. Nabavinia, M. Reza, A comparative investigation on removal performances of commercial activatedcarbon, chitosan biosorbent and chitosan/activated carbon composite for cadmium, Chem. Eng. J. 193–194 (2012) 276–282.

[21] A. Nassereldeen, A. Muataz, A. Abdullah, E. Mohamed, M.D. Alam, N. Yahya, Kinetic adsorption of application of carbon nanotubes for Pb(II) removal from aqueous solution, J. Environ. Sci. 21 (2009) 539–544.

[22] A. Razi, M. Atieh, N. Girun, T. Chuah, M. Sadig, D. Biaka, Effect of multi wall carbon nanotubes (MWCNTS) on the mechanical properties of natural rubber, J. Fullerenes, Nanotubes and Carbon Nanostruct. 14(4) (2006) 641–649.

[23] A. Muataz, F. Ahmadun, C. Guan, E. Mahdi, A. Rinaldi, Effect of reaction temperature on the production of carbon nanotubes, NANO: Brief Rep. Rev. 1(3) (2006) 251–257.

[24] G. Nazlia, A. Fakhru'l-Razi, A. Suraya, A. Muataz, Multi-wall carbon nanotubes/styrene butadiene rubber (SBR) nanocomposite, J. Fullerenes, Nanotubes, Carbon Nanostruct. 15(3) (2007) 207–214.

[25] A. Muataz, N. Nazif, Y. Faridah, M. Fettouhi, C. Ratnam, M. Al-Harthi, F. Abu-Ilawi, K. Mohammed, A. Al-Amer, Radiation vulcanization of natural rubber latex loaded with carbon nanotubes, Fullerenes, Nanotubes, Carbon Nanostruct. 18(1) (2010) 56–71.

[26] A. Muataz, M. Fettouhi, A. Al-Mammum, N. Yahya, Lead removal by using carbon nanotubes, Int. J. Nanopart. 2(1–6) (2009) 329–338.

[27] A. Muataz, O. Bakather, B. Tawabini, A. Bukhari, M. Khaled, M. Al-Harthi, M. Fettouhi, F. Abuilaiwi, Removal of chromium (III) from water by using modified and nonmodified carbon nanotubes, J. Nanomater. 2010(2010) 1–9.

[28] R. Leyva-Ramos, J.R. Rangel-Mendez, J. Mendoza-Barron, L. Fuentes-Rubio, R. Guerrero-Coronado, Adsorption of cadmium (II) from aqueous solution onto activated carbon, Water Sci. Technol. 35 (1997) 205–211.

[29] M. Mehrasbi, Z. Farahmandkia, B. Taghibeigloo, A. Taromi, Adsorption of lead and cadmium from aqueous solution by using almond shells, Water Air Soil Pollut. 199(1–4) (2009) 343–351.

[30] A. Tajar, T. Kaghazchi, Adsorption of cadmium from aqueous solutions on sulfurized activated carbon prepared from nut shells, J. Hazard. Mater. 165 (2009) 1159–1164.

[31] P. Ricou-Hoeffer, I. Lecuyer, P. Le, Experimental design methodology applied to adsorption of metallic ions onto fly ash, Water Res. 35(4) (2001) 965–976.

[32] R. Leyva, J. Rangel, J. Mendoza, L. Fuentes, R. Guerrero, Adsorption of cadmium(II) from aqueous solution on activated carbon, Water Sci. Technol. 35(7) (1997) 205–211.

[33] G. Vukovi, A. Marinkovi, M. Oli, M. Risti, R. Aleksi, A. Peri, P. Uskokovi, Removal of cadmium from aqueous solutions by oxidized and ethylenediamine functionalized multi-walled carbon nanotubes, Chem. Eng. J. 157 (2010) 238–248.

[34] S. Nomanbahay, K. Palanisamy, Removal of heavy metals from industrial waste water using chitosan coated oil palm shell charcoal, Electron. J. Biotechnol. 8 (2005) 43–53.

[35] K. Bhattacharyya, S. Gupta, Pb (II) uptake by kaolinote and montmorillnite in aqueous medium: Influence of acid activation of the clays, Colloids Surf. A 277 (2007) 191–200.

[36] F. Amalya, A. Zaharin, Experimental determination of Cd^{2+} adsorption mechanism on low-cost biological waste, Front. Environ. Sci. Eng. 7(3) (2013) 356–364.